

# Comparative Study of the Adhesion, Friction, and Mechanical Properties of CF<sub>3</sub>- and CH<sub>3</sub>-Terminated Alkanethiol Monolayers

Jack E. Houston,<sup>\*,||</sup> Christopher M. Doelling,<sup>§</sup> T. Kyle Vanderlick,<sup>§</sup> Ying Hu,<sup>‡</sup> Giacinto Scoles,<sup>‡,#</sup> Irmgard Wenzl,<sup>†</sup> and T. Randall Lee<sup>†</sup>

Sandia National Laboratory, Albuquerque, New Mexico 87185, Department of Chemical Engineering, Princeton University, Princeton, New Jersey 08540, Department of Chemistry, Princeton University, Princeton, New Jersey 08540, Department of Chemistry, University of Houston, Houston, Texas 77204, and International School for Advanced Studies and Elettra Synchrotron Laboratory, Trieste, Italy

Received December 15, 2004. In Final Form: February 8, 2005

We report the results of a direct comparison of the adhesion, friction, and mechanical properties between alkanethiol self-assembled monolayer films terminated by either CH<sub>3</sub> or CF<sub>3</sub> end groups using both interfacial force (IFM) and atomic force (AFM) microscopies. The purpose of this work is to gain insight into the detailed origins of the differing frictional behavior previously observed with AFM. The IFM results reveal an increased adhesive interaction for the CF<sub>3</sub>-terminated film due to the highly polar nature of the end groups. In agreement with earlier studies, the AFM results show two linear regions with differing frictional slopes for the CH<sub>3</sub>-terminated film but only a single slope for the CF<sub>3</sub>-terminated film. We contrast the differences between these techniques, ~100 times smaller tips for the AFM, and discuss the role of the mechanical properties, the increased adhesive interaction, and the amount of disorder present in the film in creating differences in frictional behavior between the two systems. We conclude that increased adhesion for the CF<sub>3</sub>-terminated film plays an important role in the observed differences in frictional behavior, while the differences between the two techniques can be traced to the different tip sizes and the consequent responses to the presence of disorder in the films.

## Introduction

Self-assembled monolayers (SAMs) have received considerable recent attention as molecular-level lubricants in, for example, micro-electromechanical systems (MEMS).<sup>1</sup> SAMs have been demonstrated to solve the “stiction” problem by both reducing interfacial adhesion and providing very low coefficients of friction.<sup>2</sup> In addition, efforts aimed at solving the problem of long-term stability have been addressed through specific tailoring of the molecular bonding to normal SiO<sub>x</sub> MEMS surfaces and have shown great promise.<sup>3,4</sup> Of particular interest as tribological films have been SAMs terminated by fluorocarbon groups because of their inert nature and enhanced thermal stability. Surprisingly, however, fluorocarbon films were shown to actually produce higher coefficients of friction in atomic force microscopy (AFM) studies,<sup>5</sup> and considerable subsequent work has been aimed at determining the molecular origin of this increase.<sup>6</sup> Although a variety of rationalizations have been discussed, the most widely

accepted conclusion has been that the increased van der Waals radius of the fluorine groups (~45%) causes a steric disruption of the order of the molecular surface giving rise to an increase in friction.<sup>5,6</sup>

In the present paper, two similar but complementary techniques are applied to compare directly the details of the mechanical, adhesive, and frictional properties of SAMs terminated by trifluoromethyl (CF<sub>3</sub>) groups with those terminated by methyl (CH<sub>3</sub>) groups, henceforth referred to as CF<sub>3</sub> and CH<sub>3</sub> films, respectively. The first is interfacial force microscope (IFM)<sup>7,8</sup> which is quantitative, mechanically stable, and able to determine both the normal and frictional forces over the entire range of the interfacial interaction, including both the contact and noncontact regions. Results are shown for a 2 μm tungsten tip interacting with C<sub>16</sub> alkanethiol molecules assembled on gold(111) single-crystal surfaces and include normal force vs relative tip displacement upon both approach and withdrawal, frictional force vs normal force and, relative contact–potential–difference (CPD) measurements for both films.

The stability of the IFM sensor permits the interfacial and frictional forces to be characterized over the entire range of the interaction. In addition, the larger tip used in the IFM experiments allows a better averaging of molecular properties without the high-strain effects seen with the AFM technique, which operates with tip sizes in the tens of nanometer range. On the other hand, the AFM enables one to study the frictional properties at a smaller

\* Author to whom correspondence should be addressed. E-mail: jehoust@sandia.gov.

<sup>||</sup> Sandia National Laboratory.

<sup>§</sup> Department of Chemical Engineering, Princeton University.

<sup>‡</sup> Department of Chemistry, Princeton University.

<sup>†</sup> University of Houston.

<sup>#</sup> International School for Advanced Studies and Elettra Synchrotron Laboratory.

(1) Maboudian, R.; Ashurst, W.; Carraro, C. *Sensors Actuators, A* **2000**, *82*, 219.

(2) Srinivasan, U.; Houston, M.; Howe, R.; Maboudian, R. *J. MEMS Syst.* **1998**, *7*, 252.

(3) Jun, Y.; Boiadjev, V.; Major, R.; Zhu, X. Y. *Proc. SPIE* **2000**, *4175*, 113.

(4) Major, R. C.; Kim, H. I.; Houston, J. E.; Zhu, X. Y. *Tribol. Lett.* **2003**, *14*, 237.

(5) Kim, H. I.; Koini, T.; Lee, T. R.; Perry, S. S. *Langmuir* **1997**, *13*, 7192.

(6) Kim, H. I.; Graupe, M.; Oloba, O.; Koini, T.; Imaduddin, S.; Lee, T. R.; Perry, S. S. *Langmuir* **1999**, *15*, 3179.

(7) Joyce, S. A.; Houston, J. E. *Rev. Sci. Instrum.* **1991**, *62*, 710.

(8) Houston, J. E. *Interfacial Force Microscopy: Selected Applications. In Applied Scanning Probes*; Bhushan, B., Fuchs, A. H., Hosaka, S., Eds.; Springer-Verlag: Berlin, Heidelberg, 2004; p 41.

scale, which can present distinct advantages for certain purposes; moreover, AFM has been widely used to study the frictional properties of molecular monolayers on surfaces. In addition to the results mentioned before,<sup>5,6</sup> other AFM results include studies of the pressure-dependent structural and frictional properties of *n*-alkanethiols on gold.<sup>9</sup> These studies have found that a critical threshold force exists that induces a structural transition in the SAM, the value of which is related to the tip radius. This finding clearly illustrates the high-strain effects inherent in the use of this technique for probing film properties at the molecular level. Therefore, before and after this transition, the slope of the lateral deflection of the AFM tip, which is proportional to the frictional force, versus the normal force is different, being larger after the transition because of the increased amount of disorder due to tip-penetration effects. In addition, SAMs assembled with shorter molecules show larger friction, which is due to the fact that they are less well ordered, i.e., more liquidlike, than the films made of longer molecules.<sup>10</sup>

AFM measurements of friction can also be complicated by other factors, such as crosstalk between the lateral and vertical signals, laser spot positioning on the detector, and the shape and coating of the AFM cantilevers. Because of these problems, even though a sizable effort has been made to calibrate the torsional spring constant and calculate absolute frictional properties of surfaces,<sup>11,12</sup> most of this work assumes that when comparing two different surfaces, all of the uncontrollable parameters, e.g., the chemical composition of the tip, remains constant. To circumvent the latter problem, we use here a technique referred to as "Dip-Pen Nanografting" (DPNG).<sup>13</sup> DPNG is a combination of dip-pen nanolithography<sup>14</sup> and nanografting.<sup>15</sup> Basically, an AFM tip is first soaked in an ethanolic solution of thiol molecules (in our case CF<sub>3</sub>-terminated thiols). After the ethanol is allowed to evaporate, the tip is mounted and a CH<sub>3</sub>-terminated SAM surface is then scanned at a minimum force. After an appropriate area is selected, the force is increased to a level just capable of removing the original CH<sub>3</sub> molecules, which leads to replacement with the fluorinated molecules originally loaded onto the tip. The CF<sub>3</sub> molecules self-assemble onto the freshly exposed gold surface. Afterward, both height and frictional images, in trace and retrace directions, are captured. Because the presence of the original host layer on the gold surface limits the diffusion of the grafted thiol molecules, a significant increase in pattern resolution is achieved, and more importantly to us here, by using the same tip to study two different SAMs in the same scan, accurate height and frictional properties can be meaningfully studied and compared.

## Experimental Section

The unique capabilities of IFM have been described in detail elsewhere.<sup>7,8</sup> This technique allows the simultaneous measurement of normal and frictional forces as a function of relative tip displacement while maintaining the sensor stability over the entire force/displacement range. While IFM is sensitive to both

normal and lateral tip forces, these are not independently measured. To separate the two, the sample is laterally dithered by a sine-wave oscillator at 100 Hz with an amplitude of ~2.5 nm, which corresponds to a maximum lateral speed of ~1600 nm/s. This approach allows the lateral and normal forces to be separated in the frequency domain using a lock-in amplifier. Data are presented as both frictional force plotted as a function of normal force and frictional and normal forces plotted as a function of relative interfacial separation.

Quantitative data were collected in a differential mode, keeping the experimental conditions the same (identical probe tip and sensor) for a direct comparison of the behavior of the two films. The metal probe tips were formed by electrochemically etching 200  $\mu$ m tungsten and gold wires to parabolic shapes having radii of ~2  $\mu$ m, as characterized by scanning electron microscopy. As the tip of the IFM is approximately 2 orders of magnitude larger than that used in the AFM, the tip is considerably more robust with respect to wear than that used in AFM. All IFM experiments were performed under a blanket of dry nitrogen (RH < 5%) at room temperature and atmospheric pressure.

Contact potential difference (CPD) data were obtained by holding the IFM tip at a constant interfacial separation of ~20 nm while recording the resulting electrostatic force created by a ramped voltage ( $\pm 10$  V) applied to the substrate with the gold reference tip grounded. The electrostatic force varies as the square of the applied voltage, and the CPD value corresponds to an applied voltage resulting in no electrostatic force. Data were taken at several locations on the surface, least-squares fit to a parabolic function, and the CPD results averaged to obtain a more precise value. The CPD is, of course, the applied potential necessary to force the "vacuum levels" for the two surfaces to have the same value. Since gold is the common reference surface, the difference between the CPD values for the two films yields their mutual work-function difference.

The two alkanethiol molecules, hexadecanethiol for the CH<sub>3</sub> film and 16,16,16-trifluorohexadecanethiol for the CF<sub>3</sub> film, are identical, differing only in the functionality of their end groups. The methyl-terminated molecules were obtained commercially from Sigma-Aldrich, while the fluorinated molecules were synthesized as described previously.<sup>16</sup> Both monolayer films used in the IFM experiments were self-assembled from 1 mM ethanolic solutions on the (111)-orientated facets of a single-crystal gold substrate, prepared by flame annealing 99.99% pure gold wire.<sup>17</sup>

The AFM experiments were carried out as described above with a Veeco Nanoscope IIIa apparatus. The cantilevers are made of oxide-sharpened silicon nitride, and the spring constant is given by the manufacturer to be 0.12 N/m. The frictional spring constant is calculated based on a model also provided by the manufacturer. The CH<sub>3</sub>-terminated films were prepared by the self-assembly of CH<sub>3</sub>(CH<sub>2</sub>)<sub>15</sub>SH molecules from a 0.1 mM 2-butanol solution onto a thermally evaporation-deposited gold (111) surface on a mica substrate with assembly times in excess of 24 h. Past experience has shown that this low-concentration, long-term method consistently produces high-quality films. The DPNG procedure utilized CF<sub>3</sub>-(CH<sub>2</sub>)<sub>15</sub>-SH molecules from the same source as those used in the IFM experiments. After the pattern formation, the imaging forces were increased step by step and height images and frictional images in both trace and retrace direction were captured. The subtraction of the trace and retrace frictional images were then divided by two. Averages of multiple-reading, frictional data were recorded as photodiode output in volts and the conversion to lateral force utilized the procedure outlined by Sader<sup>11</sup> with cantilever parameters from the manufacturer's specifications. The repeatability of the measurements was checked by taking data first at a moderate load then at a higher value followed by a return to the original load value and repeating. The agreement was found to be well within the normal signal-to-noise spread. It should be pointed out that after grafting the tip remains coated with the fluorinated molecules. However, since the comparison between the two molecules is made under

(9) Lio, A.; Morant, D. F.; Ogletree, D. F.; Salmeron, M. *J. Phys. Chem. B* **1997**, *101*, 4767.

(10) Xiao, X.; Hu, J.; Charych, D. H.; Salmeron, M. *Langmuir* **1996**, *12*, 235.

(11) Sader, J. E. *Rev. Sci. Instrum.* **2003**, *74*, 2438.

(12) Ogletree, D. F.; Carpick, R. W.; Salmeron, M. *Rev. Sci. Instrum.* **1996**, *67*, 3298.

(13) Amro, N. A.; Xu, S.; Liu, G. Y. *Langmuir* **2000**, *16*, 3006.

(14) Piner, R. D.; Zhu, J.; Xu, F.; Hong, S.; Mirkin, C. A. *Science* **1999**, *283*, 661.

(15) Xu, S.; Liu, G. Y. *Langmuir* **1997**, *13*, 127.

(16) Graupe, M.; Koini, T.; Wang, V. Y.; Nassif, G. M.; Colorado, R.; Villazana, R. J.; Dong, H.; Miura, Y. F.; Shmakova, O. E.; Lee, T. R. *J. Fluorine Chem.* **1999**, *93*, 107.

(17) Schneir, J.; Sonnenfeld, R.; Marti, O.; Hansma, P. K.; Demuth, J. E.; Hamers, R. *J. Appl. Phys.* **1988**, *63*, 717.

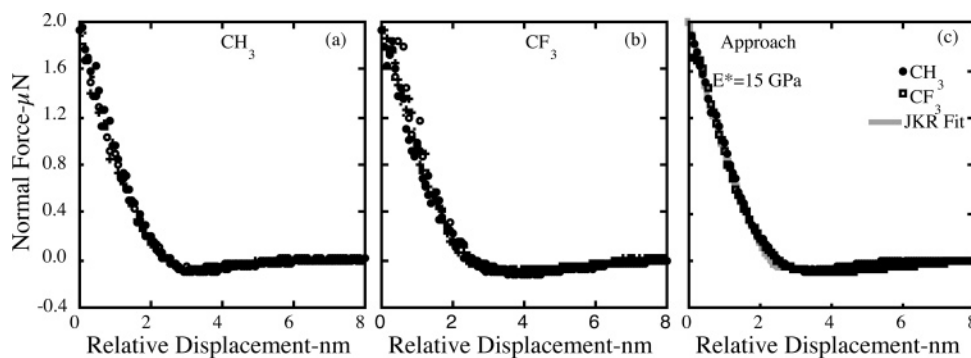


**Figure 1.** (a) and (b) The approach portion of the normal force vs relative tip displacement IFM profiles for the  $\text{CH}_3$ - and  $\text{CF}_3$ -terminated films taken by at least five different locations on the surface, and (c) the averaged data of (a) and (b) plotted together, along with a fit according to the JKR model shown as the gray solid line.

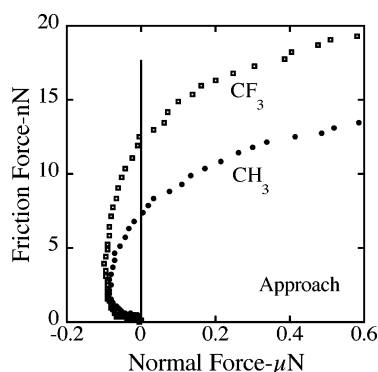


**Figure 2.** Averaged IFM data of frictional force vs normal force comparing the behavior of the  $\text{CH}_3$ - and  $\text{CF}_3$ -terminated films. Negative normal forces are attractive, while positive values are repulsive.

the same tip condition, we assume that this does not affect the relative conclusions.

## Results

**IFM Results.** Figure 1a and b illustrates the force vs relative displacement data corresponding to the approach portion of the force profiles for both films taken at several locations on the surface. The small scatter justifies data averaging, the results of which are shown as a composite plot in Figure 1c. The results for the two films are virtually identical in the repulsive region of Figure 1c, with small differences in the light and noncontact areas. Also shown in Figure 1c is a fit to the simple JKR contact-mechanics model<sup>18</sup> (grey solid line), again illustrating the similarities in mechanical behavior in the repulsive region. The reduced modulus obtained from this fit corresponds to a value of  $\sim 15 \text{ GPa}$ . However, it should be noted that this value is only obtained over a limited displacement range and is exaggerated by the level of strain involved.<sup>8</sup> In addition, the mechanical behavior of the films is highly nonlinear at higher forces and eventually reflects the composite modulus of the gold substrate and tungsten tip.

In Figure 2, we show the frictional vs normal force curves for the  $\text{CF}_3$  and  $\text{CH}_3$  films, again, averaged over several different locations on the sample. The most dramatic difference in the two responses is the sharp rise in friction in the attractive regime for the  $\text{CF}_3$  film. At higher forces, the frictional behavior is similar; however, the initial offset contributes considerably to the overall  $\sim 45\%$  increase in friction at the higher loads. This increase in friction for

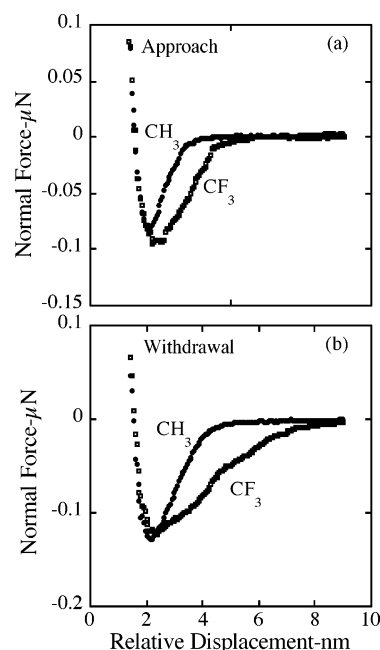


**Figure 3.** (a) The averaged IFM data of Figure 1c plotted with a normal-force scale expanded by approximately a factor of 10 and (b) similar data corresponding to the withdrawal portion of the force profiles.

the  $\text{CF}_3$  film is in agreement with earlier results. However, it is considerably less than the approximately 3-fold increase reported in the earlier AFM studies.<sup>5,6</sup> In addition, the AFM studies usually reported a linear variation in friction with normal load, whereas here, the behavior is more reminiscent of the contact-area dependence characterized, for example, by Carpick et al.<sup>19</sup>

In Figure 3, we show the averaged data of Figure 1c, along with that corresponding to tip withdrawal, with the y scale magnified by approximately a factor of 10. Upon approach, there is only a small difference in the maximum attractive force for the two films, and the  $\text{CF}_3$  film has an increased range of interaction by about 1 nm. Upon withdrawal, the maximum attractive forces for both films are virtually identical and somewhat larger than the approach values. The maximum attractive force corresponds to the so-called "pull-off force" when measured by normal displacement detectors, such as that used in the AFM and surface forces apparatus,<sup>20</sup> and again, this latter result agrees with the earlier studies.<sup>21</sup>

(18) Johnson, K. L.; Kendall, K.; Roberts, A. D. *Proc. R. Soc. London* **1971**, A324, 301.

(19) Carpick, R. W.; Agrait, N.; Ogletree, D. F.; Salmeron, M. *Langmuir* **1996**, 12, 3334.

(20) Israelachvili, J. *Chemtracts* **1989**, 1, 1.

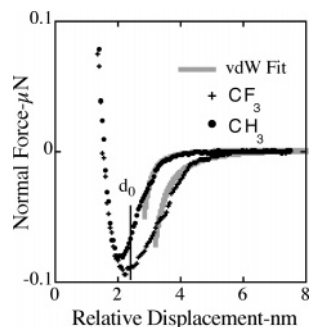


**Figure 4.** The IFM data of Figure 3a with fits according to the parametrized van der Waals relationship. The solid line marked  $d_0$  indicates the common point corresponding to the location of the surface of the two films, according to the fits, with the curves aligned according to the common behavior in the repulsive portion of the data. The Hamaker constants resulting from these fits are  $3.5 \times 10^{-20}$  and  $13.5 \times 10^{-20}$  J for the  $\text{CH}_3$ - and  $\text{CF}_3$ -terminated films, respectively.

In Figure 4, we show the data of Figure 3b along with fits (solid gray lines) using the van der Waals relationship,<sup>22</sup>

$$\frac{F}{R} = \frac{A}{6(d - d_0)^2} \quad (1)$$

where  $R$  is the tip radius,  $A$  is the Hamaker constant for the tip/substrate combination, and  $d_0$  is the point corresponding to the location of the film surface. These fits were made with the same value of  $d_0$  (solid vertical line in the figure) and  $A$  values of  $3.5 \times 10^{-20}$  J for the  $\text{CH}_3$  film and  $13.5 \times 10^{-20}$  J for the  $\text{CF}_3$  film, which is a factor of almost four larger than that for  $\text{CH}_3$  film. Thus, the interaction range appears extended for the fluorinated film because of its larger interaction strength.

Since fluorine is the most electronegative element in the periodic table, the  $\text{CF}_3$  groups can be expected to present a field of dipoles with significant components normal to the surface, as was pointed out in early work by Zisman and co-workers.<sup>23,24</sup> Such a dipole field, with negative charges normal to the surface, will give rise to a significant increase in the work function of the  $\text{CF}_3$  film. To evaluate this phenomenon, we show in Figure 5 a direct measurement of the CPD for the two films relative to a gold tip. The CPD for the  $\text{CH}_3$  film is slightly less than  $-1.1$  V, and the value for the  $\text{CF}_3$ -terminated film is slightly less than 0 V. Thus, the work function for the gold/thiol/ $\text{CH}_3$  system is a bit more than a volt less than that of gold ( $\sim 4.5$  V), while that for the gold/thiol/ $\text{CF}_3$  system is virtually equal to that of gold. The difference between these two CPD values is the increase in work function due simply to the substitution of the highly polar  $\text{CF}_3$  group for that of  $\text{CH}_3$ , indicating the strong surface-normal component of the dipole moment of the  $\text{CF}_3$  moieties.

Finally, to clarify the spatial variation of the frictional force with normal force, we show in Figure 6 a composite plot similar to Figure 4 that includes the behavior of the frictional force. We see here a measurable rise in friction in the noncontact region of the profile followed by a steep increase corresponding to the initial tip/film contact (schematically indicated by the solid vertical lines). Note

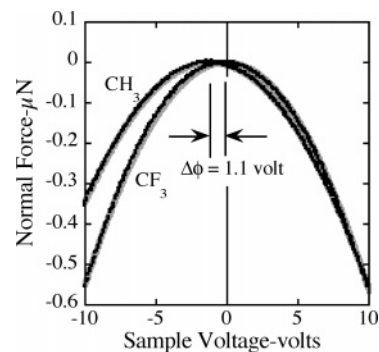


**Figure 5.** Normal forces vs voltage applied to the sample substrate (tip grounded) as measured by IFM. The force varies as the voltage squared, and the point at which the force goes to zero represents the contact potential difference (CPD) between the substrate and its film and the gold tip, i.e., where the vacuum levels of the two are the same. The difference in CPD values for the two films is  $\sim 1.1$  V.

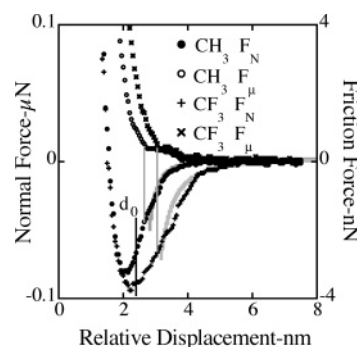


**Figure 6.** Normal and frictional forces plotted against relative displacement. Also included are the van der Waals fits and two additional gray vertical lines indicating the approximate points at which the frictional forces begin to rapidly rise. These points both appear somewhat earlier in the approach than that of the common  $d_0$  value shown in Figure 4.



**Figure 7.** AFM image ( $300 \text{ nm} \times 300 \text{ nm}$ ) depicting the relative heights for a  $\text{CF}_3$ -terminated SAM (the light colored square) nanografted into a  $\text{CH}_3$ -terminated SAM. The darker color corresponds to a lower height. The height differences between the nanografted patterns and the matrix are about  $0.2 \text{ nm}$  but ranges over several images from near zero to  $0.2 \text{ nm}$ . The image clearly shows that the grafted pattern follows the surface features of the gold step.

also that this steep rise begins a few tenths of a nanometer further out for the  $\text{CF}_3$  film relative to the  $\text{CH}_3$  film.

**AFM Results.** Figure 7 shows the results of nanografting  $\text{CF}_3-(\text{CH}_2)_{15}-\text{SH}$  molecules into a previously

(21) Graupe, M.; Koini, T.; Kim, H. I.; Garg, N.; Miura, Y. F.; Takenaga, M.; Perry, S. S.; Lee, T. R. *Mater. Res. Bull.* **1999**, *34*, 447.

(22) Israelachvili, J. *Intermolecular & Surface Forces*; Academic Press: New York, 1992.

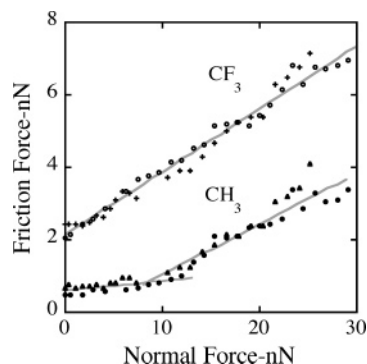


**Figure 8.** Frictional force data for the  $\text{CF}_3$ - and  $\text{CH}_3$ -terminated films versus the normal imaging force as measured by AFM. Each data point corresponds to one friction measurement and the friction values are derived from voltage readings as described in the Experimental Section. The linear least-squares fit for the friction of the  $\text{CF}_3$ -terminated film is  $F_\mu = 0.17F_N + 2.1$  over the entire force range, while for the  $\text{CH}_3$ -terminated film, it is  $F_\mu = 0.026F_N + 0.6$  between zero and 10 nN and  $F_\mu = 0.14F_N - 0.21$  between 10 and 28 nN.

assembled  $\text{CH}_3-(\text{CH}_2)_{15}-\text{SH}$  film. More than six patterns were made, and a representative height image is presented here. The central  $\text{CF}_3$  patch is  $\sim 0.2 \pm 0.1$  nm higher than that of the background matrix. The 0.2 nm value is slightly larger than the height difference predicted on the basis of a simple geometric model, i.e., the larger  $\text{CF}_3$  groups cause the parts of the molecules near the surface to stand slightly more erect. After each pattern was made, the area with the  $\text{CF}_3$  film was imaged multiple times to study the friction versus normal force relationship, with the imaging forces increasing in the range from  $\sim 0$  to 28 nN. As shown by the data in Figure 8, the increase in friction for the  $\text{CF}_3$  film is essentially linearly dependent on the imaging force, permitting a coefficient of friction to be defined, which according to a least-squares fit, has a value of  $\sim 0.17$ . However, there is a clear slope difference for the frictional data of the  $\text{CH}_3$  film, where the coefficient measured above  $\sim 10$  nN ( $\sim 0.14$ ) is more than five times larger than that measured at the lower normal forces ( $\sim 0.026$ ).

### Discussion and Conclusions

In the averaged frictional vs normal force curves of Figure 2, the most notable difference between the behavior of the two films is the rapid rise in friction in the attractive region for the  $\text{CF}_3$  film. In fact, if the  $\text{CH}_3$  curve is shifted upward by  $\sim 6$  nN, the two curves virtually lie one on top of the other above a normal force of about  $0.07 \mu\text{N}$ . This behavior would seem logical, since, from Figure 1c, the mechanical deformation of the films is virtually identical for normal forces just above zero. Thus, the friction due to the film disturbance under reasonable repulsive mechanical contact is essentially the same. This kind of friction is usually characterized by a frictional shear strength and will vary in magnitude in direct proportion to the mechanical contact area.<sup>19,25</sup> Generally speaking, this phenomenon is what gives rise to the looping behavior of the frictional force with normal force, and in fact, such behavior can often be accurately characterized by simple contact-mechanics models.<sup>19,25</sup> However, neither of the curves presented in Figure 2 can be adequately characterized by this procedure, and the reason, in both cases, is that the frictional force is offset by a significant contribution from portions of the film that are not in actual

mechanical contact. In other words, the attractive force between the tip and film, which competes with the intrafilm van der Waals forces involved in the self-assembly, disturbs the film structure and causes a frictional energy loss. As shown in Figure 4, this attractive force is smaller for the  $\text{CH}_3$  film, but is still significant. The fact that the tip/film attractive force affects the film structure can also be seen in the small but abrupt deviation from the van der Waals fits for both films in Figure 4. Although slight, this attractive-force increase indicates that the film immediately below the tip suddenly stands up to meet the approaching tip, slightly decreasing the tip/film separation. Such behavior was not observed when a  $\text{CH}_3$  substrate film was allowed to interact with a similar film on a gold tip.<sup>25</sup> In this case, the contact-area model provided a reasonably accurate characterization. In the present case, however, the tungsten tip of the interfacial force microscope provides a considerably larger Hamaker constant for the interaction with a hydrocarbon surface than that involved for the interaction of two hydrocarbon surfaces, and the relationship between friction and contact area no longer strictly holds.

The increased strength of the Hamaker constant for the  $\text{CF}_3$  film calculated from the van der Waals fits of Figure 4 indicates the role of the Debye (or dipole/induced dipole) component of the van der Waals force arising from the strong  $\text{CF}_3$  dipole moment at the film surface.<sup>26–29</sup> The effect of this force on film structure, and thus friction, is enhanced further by the fact that it is concentrated on the end groups themselves, as opposed to distributed over the entire film by the normal distance dependence of the van der Waals force. The presence of strong surface dipoles in  $\text{CF}_3$ -terminated films is plausible given the electronegativity of the fluorine atoms (largest in the periodic table), and the influence of these dipoles on interfacial wettability has been noted.<sup>23,24,27,28</sup> Moreover, the strength of the normal component of the surface dipoles is verified by the  $\sim 1.1$  V CPD value obtained from the data of Figure 5, which is in good agreement with UV-photoemission results reported earlier.<sup>29</sup> The enhanced van der Waals force effectively increases the “area of interaction”<sup>30</sup> between the tip and film and leads to both a measurable frictional force with no mechanical contact and an additional component due to the disturbance of molecules outside the area of the *actual* mechanical contact. The effect represents a competition between the tip/film van der Waals interaction and the film–film (intrafilm) interaction, which has also been noted in recent molecular dynamics calculations.<sup>31</sup>

The friction of the  $\text{CF}_3$  films is also enhanced by a decrease in surface order<sup>32</sup> caused by the relatively large size of the  $\text{CF}_3$  groups, as well as the dipole–dipole repulsion between neighboring end groups, originally suggested by Zisman and co-workers.<sup>23,24</sup> This decreased order was given earlier as the principal reason for the increased friction for the  $\text{CF}_3$  films, but the contribution of dipole effects was dismissed because the measurements by AFM showed no increase in adhesion for the  $\text{CF}_3$ -terminated films.<sup>5,6</sup> In the present study, however, analysis

(26) Reference 22, pp 74 and 75

(27) Graupe, M.; Takenaga, M.; Koini, T.; Colorado, R.; Lee, T. R. *J. Am. Chem. Soc.* **1999**, *121*, 3222.

(28) Colorado, R.; Lee, T. R. *J. Phys. Org. Chem.* **2000**, *13*, 796.

(29) Alloway, D. M.; Hofmann, M.; Smith, D. L.; Gruhn, N. E.; Graham, A. L.; Colorado, R.; Wysocki, V. H.; Lee, T. R.; Lee, P. A.; Armstrong, N. R. *J. Phys. Chem. B* **2003**, *107*, 11690.

(30) Reference 22, p 159

(31) Harrison, J. A. private communication.

(32) Pflaum, J.; Bracco, G.; Schreiber, F.; Colorado, R.; Shmakova, O. E.; Lee, T. R.; Scoles, G.; Kahn, A. *Surf. Sci.* **2002**, *498*, 89.

(23) Shafrin, E. G.; Zisman, W. A. *J. Chem. Phys.* **1957**, *61*, 1046.

(24) Shafrin, E. G.; Zisman, W. A. *J. Phys. Chem.* **1962**, *66*, 740.

(25) Houston, J. E.; Kim, H. I. *Acc. Chem. Res.* **2002**, *35*, 547.

by IFM strongly suggests that surface dipoles both influence adhesion and contribute to interfacial friction. This apparent contradiction is discussed below in detail.

An important feature of the AFM data in Figure 8 is the dual slope of the frictional response for the CH<sub>3</sub> film. A similar dual-slope behavior was observed in some of the friction vs load plots in earlier AFM studies directly comparing CH<sub>3</sub> and CF<sub>3</sub> films, as well as a film terminated by larger isopropyl groups.<sup>6,10</sup> The cross sections for these groups has been reported to scale as 13, 19, and 23 Å<sup>2</sup> for CH<sub>3</sub>, isopropyl, and CF<sub>3</sub>, respectively.<sup>6</sup> The combination of these results suggest that the CH<sub>3</sub> surface groups remain reasonably well ordered at smaller loads with relatively few avenues for energy dissipation. With increasing load, however, the tip penetrates the film and the friction dramatically increases. Such a "transition" behavior has been explored in earlier AFM work.<sup>9</sup> A simple, qualitative description of the process can be developed by looking in detail at the molecular conformation of the layer. In the self-assembly process, the carbon chains tilt ~30° from the surface normal to maximize the intramolecular van der Waals interactions. The interaction is enhanced by nesting the methylene groups in a "ratcheted" structure, further increasing their packing. At low tip loads, movement of the molecules is restricted so the tip-induced film strain is limited and the avenues for energy dissipation are minimal. However, under higher stresses, the chains can increase the level of strain by sliding, or ratcheting, down the zigzag conformation of the carbon atoms. One ratchet step would increase the molecular tilt by an additional ~25°, which would involve an increase in film strain of about 28% at a film deformation of ~0.7 nm. Such a process would lead to a dramatic increase in the avenues for energy dissipation by, for example, the creation of gauche conformations and related defects. With the small AFM tip and only about 200 molecules involved in the contact, a normal force of ~10 nN is apparently sufficient to overcome the energy barrier involved in the ratchet step, and the result is a dramatic increase in coefficient of friction.

The same two-slope behavior has been observed in previous IFM measurements for a methyl-terminated C<sub>16</sub> monolayer assembled on single-crystal gold(111) but at higher loads.<sup>33</sup> In this case, a tungsten tip was used with a 190 nm radius, which involved about 2000 molecules within the contact. The friction varied linearly with load, and the break in the friction occurred at about 4 μN, where the slope increased from a value of ~0.004 to ~0.07. This work also demonstrated that the linear behavior of the frictional force with load, which on smooth surfaces should increase as the contact area increases,<sup>25</sup> is the result of the fact that the energy dissipation involves a thin film, where only a finite level of strain can be obtained. This limitation alters the relationship between energy dissipation in the film and the applied load. It is found that IFM results for molecular films always appear linear at higher loads.<sup>33</sup> AFM studies of molecular-level friction generally report linear behavior throughout the repulsive regime. Clearly, the zero-load strain is sufficient to place the repulsive region under the thin-film, constant-slope condition. No breaks in frictional behavior are observed in the data of Figure 2, and the results have a familiar contact-area related appearance, indicating that the strain levels in the IFM experiments are considerably less than those involved in the AFM experiments over the range of forces shown.

Considering the combination of our present findings, we conclude that the adhesive interaction between the tip and film, along with the very small tips used, is sufficiently

strong in the AFM measurements to produce the high strain, linear-frictional behavior in the repulsive region. In addition, this effect gives a plausible explanation for the contrasting friction results seen for the CH<sub>3</sub> and CF<sub>3</sub> films. For the small end groups of the CH<sub>3</sub> films, surface order is high and low-load friction is low. Increasing the load eventually gives rise to an internal structural transition leading to higher friction. A larger nonpolar group, such as isopropyl, gives similar two-stage friction with both sections having higher slopes than seen for the CH<sub>3</sub><sup>6</sup> because of a further decrease in surface order. In contrast, the CF<sub>3</sub> film combines a larger end group with an increase in adhesion by almost a factor of 4, *as measured by IFM for the interaction between the films and a tungsten tip*. We suggest that this increase in adhesive force is sufficient to offset the point of zero applied load to a position above the low-friction region to give a single high-slope frictional behavior.

To support the above picture, we make a crude calculation of the maximum van der Waals force, using the Hamaker constants of Figure 4 for both films, and assume that the minimum separation in the van der Waals relation of eq 1 is the "universal value" of 0.165 nm described by Israelachvili.<sup>34</sup> For AFM, the maximum adhesive forces are 4.3 and 16.5 nN, and for IFM, these values are 0.43 and 1.7 μN for the CH<sub>3</sub> and CF<sub>3</sub> films, respectively. If we assume that the total force on the tip at the break point for the CH<sub>3</sub> film in AFM is ~14 nN (applied plus maximum van der Waals), then the total force at the zero of applied force for the CF<sub>3</sub> film is above the frictional break-point force. The argument is further strengthened by the fact that in the earlier CH<sub>3</sub>/isopropyl/CF<sub>3</sub> comparison,<sup>6</sup> (1) the break point for the intermediate sized isopropyl groups occurred at a smaller force than for CH<sub>3</sub>, which would indicate that it would even be smaller for the larger CF<sub>3</sub> groups, and (2) all three slopes in the high-load region were found to have about the same value, suggesting that the end-group size was playing only a minor role.<sup>6</sup> A similar situation holds for the IFM CF<sub>3</sub> behavior of Figure 2. However, the argument is more difficult to make here because the behavior is more contact-area related, involving the unique mechanics of the films in the attractive region (see below).

We emphasize, however, that the multislope behavior in AFM measurements, such as those illustrated in Figure 8, is not always observed and is rarely seen for films comprised of shorter molecular lengths.<sup>10</sup> The quality of the self-assembly processing appears to be a critical feature. In our present AFM results, the lower thiol concentration and extended exposure times appear to produce consistently a monolayer that is densely packed with few defects. Although the conclusions reached from our comparison between the present AFM results and those obtained earlier for CH<sub>3</sub>-, CF<sub>3</sub>-, and isopropyl-terminated SAMs is very provocative,<sup>6</sup> confirmation will require a more-coordinated and direct study using the same assembly procedure with careful attention to the film quality.

Finally, we note from Figure 3b that the maximum attractive force (the so-called "pull-off force") is measured to be approximately the same for both the CH<sub>3</sub> and CF<sub>3</sub> films. This finding is in agreement with earlier AFM results<sup>5,6,35</sup> and was taken in that work to be evidence that the work of adhesion for the two films is the same. However, it is clear from the IFM data in Figure 4 that

(33) Kiely, J. D.; Houston, J. E. *Langmuir* **1999**, *15*, 4513.

(34) Reference 22, p 203.

(35) Burnham, N. A.; Dominguez, D. D.; Mowery, R. L.; Colton, R. *J. Phys. Rev. Lett.* **1990**, *64*, 1931.

the energy of adhesion, the work done in pulling the surfaces apart from the equilibrium point (the zero of normal force), is considerably larger for the  $\text{CF}_3$  film relative to that for the  $\text{CH}_3$  film. In fact, integrating the two curves results in a ratio of almost a factor of 2. This result emphasizes an extremely important point. The relationship between the “pull-off force” and the work of adhesion has only been quantitatively established for linearly elastic solids by, for example, the JKR and DMT procedures.<sup>36</sup> The restrictions placed on the material interactions by these models are *seldom* met in general adhesion studies and would be of value even qualitatively *only* under the assurance that the mechanical properties of the interaction remain the same for all situations to be compared. The fact that the adhesive interaction can increase without changing the maximum adhesive force is tied up in the complex contact mechanics of the molecular films under the action of long-range forces, especially under light loads. This behavior is illustrated in recent molecular simulations of the stress–strain behavior for SAM films involving molecules of differing lengths.<sup>37</sup>

---

(36) Maugis, D. J. *Colloid Interface Sci.* **1992**, *150*, 243.

(37) Chandross, M.; Grest, G. S.; Stevens, M. J. *Langmuir* **2002**, *18*, 8392.

**Acknowledgment.** The authors wish to thank Professor Scott Perry for helpful discussions regarding the data in this manuscript. The portion of the work done at Sandia was supported by the Department of Energy, Basic Energy Sciences, Division of Materials Sciences. Sandia is a multi-program laboratory operated by Sandia Corporation, a Lockheed Martin Company, for the U.S. Department of Energy’s National Nuclear Security Administration under Contract No. DE-AC04-94AL85000. A portion of the work at Princeton University was funded through the National Science Foundation via the Materials Research Science and Engineering program Grant No. DMR 0213706, and Y. H. gratefully acknowledges support from the Department of Energy, Basic Energy Sciences, Division of Materials Sciences under Contract No. DE-FG02-93ER45503. The work at the University of Houston was supported by the Texas Advanced Research Program (003652-0307-2001) and the Robert A. Welch Foundation (Grant No. E-1320). I.W. gratefully acknowledges support from the “Fonds zur Foerderung der wissenschaftlichen Forschung” (FWF) in the form of an “Erwin-Schroedinger” Postdoctoral Fellowship (J1804-CHE).

LA046901T